Littoral landforms of Lake Hulun and Lake Buir (China and Mongolia)
Wind-driven hydro-sedimentary dynamics and resulting clastics distribution

Wang, Li; Schuster, Mathieu; Xin, Shi Wei; Zainescu, Florin; Xue, Xin Yu; Storms, Joep; May, Jan Hendrik; Nutz, Alexis; van der Vegt, Helena; Bozetti, Guilherme

DOI
10.1016/j.jop.2024.03.002

Publication date
2024

Document Version
Final published version

Published in
Journal of Palaeogeography

Journal of Palaeogeography, 2024, 13(2): 309—326 (00333)

Available online at www.sciencedirect.com

ScienceDirect

journal homepage: http://www.journals.elsevier.com/journal-of-palaeogeography/

Facies analysis and sedimentary environments

Littoral landforms of Lake Hulun and Lake Buir (China and Mongolia): Wind-driven hydro-sedimentary dynamics and resulting clastics distribution

Li Wang [a,b], *Mathieu Schuster* [b,*], *Shi-Wei Xin* [c], *Florin Zainescu* [d,i], *Xin-Yu Xue* [e,f], *Joep Storms* [f], *Jan-Hendrik May* [g], *Alexis Nutz* [d], *Helena van der Vegt* [h], *Guilherme Bozetti* [b], *Zai-Xing Jiang* [a,**]

[a] *School of Energy Resources, China University of Geosciences (Beijing), Beijing, 100083, China*
[b] *Université de Strasbourg, CNRS, ENGEES, Institut Terre et Environnement de Strasbourg, UMR 7063, 5 Rue Descartes, Strasbourg, France*
[c] *Tamsag Mongolia (XIX) Ltd., PetroChina, Daqing 163000, China*
[d] *CEREGE, Aix-Marseille Université, CNES, IRD, Collége de France, INRA, Aix en Provence, France*
[e] *School of Marine Science, Sun Yat-sen University, Zhuhai 519083, China*
[f] *Delft University of Technology, Department of Geoscience and Engineering, Delft, the Netherlands*
[g] *School of Geography, Earth and Atmospheric Sciences, University of Melbourne, 253 Elgin St., Carlton, VIC 3053, Australia*
[h] *Deltares, Delft, the Netherlands*
[i] *SCMF, Faculty of Geography, University of Bucharest, 1 N. Balcescu Blv., Bucharest, Romania*

Abstract Two rectangular-shaped lakes, Lake Hulun and Lake Buir, located at the boundary between China and Mongolia, only c. 75 km apart and therefore experiencing similar wind fields, have been studied based on satellite images and field surveys in order to compare their geomorphological and sedimentological characteristics. The wind-driven hydrodynamics, which have a significant effect on the development of littoral landforms and on sediment distribution, have been discussed for the two similar lakes that experienced a prevailing wind perpendicular to their long axis. A conceptual model related to wind-driven water bodies and sediment distribution is proposed. Wave-influenced to wave-dominated deltas, beaches, spits, and eolian dune deposits develop around these two lakes, with a strikingly similar distribution pattern. These features locally inform the longshore drift and help reconstruct the water circulation induced by wind forcing. Under the NW prevailing wind regime, the spits developed on the SW coast with a NW—SE extension, which was influenced by the NW—SE longshore currents. The same influence was observed in the delta extension in the NE area. The

* Corresponding author.
** Corresponding author.
E-mail addresses: mschuster@unistra.fr (M. Schuster), jiangzx@cugb.edu.cn (Z.-X. Jiang).
Peer review under responsibility of China University of Petroleum (Beijing).
https://doi.org/10.1016/j.jop.2024.03.002

differences lie in the presence of fan deltas in the NW region of Lake Hulun, but not in Lake Buir. Additionally, the width of the beach and eolian deposits on the downwind coast of Lake Hulun is three times greater than that of Lake Buir which were caused by the differences in sediment supply and wind fetch between the two lakes. Lake Hulun and Lake Buir provide two reliable examples to understand the relationship among the wind field, provenance, hydrodynamics, landforms, and asymmetrical distribution of clastics in elongated lakes. They also represent relevant modern analogs, which may also be of guiding significance to wind-driven sand body prediction in lacustrine basins.

Keywords Wind-driven lakes, Fetch, Sedimentary facies, Hydrodynamics, Geomorphology, Spits, Shoreline, Lake Hulun, Lake Buir

Received 6 May 2023; revised 15 December 2023; accepted 16 February 2024; available online 18 March 2024

1. Introduction

Over the past decade, wind-driven hydrodynamics in lakes have become a topic of increasing interest to understand the distribution of clastics in continental sedimentary basins (Nutz *et al.*, 2015; Jiang, 2018; Jiang *et al.*, 2018; Schuster and Nutz, 2018; Liu *et al.*, 2021; Xue *et al.*, 2021). A great number of wind-driven lakes like Lake Saint-Jean, Lake Qinghai, and Lake Turkana have been identified and studied all over the world (Nutz *et al.*, 2015, 2018; Jiang, 2018; Zăinescu *et al.*, 2023). This reveals that sediment distribution, hydrodynamics, and landforms associated with these lakes are dominantly influenced by the wind field (Carson and Hussey, 1962; Schuster *et al.*, 2005; Bouchette *et al.*, 2010; Nutz *et al.*, 2015; May *et al.*, 2022), ultimately highlighting the significant role of waves and currents in shaping the shorelines.

Even though wave-related geomorphic and sedimentary processes are generally associated with marine settings and more rarely with lakes (Davis and Hayes, 1984; Clifton, 2006; Schwartz, 2012; Schuster and Nutz, 2018), significant waves develop when the wind blows across any water surface and consequently plays an important role in controlling sediment distribution and landform evolution in lakes as well (Allan and Kirk, 2000; Pochat *et al.*, 2005; Keighley, 2008; Nordstrom and Jackson, 2012; Andrews and Hartley, 2015). To address this deficiency and improve the understanding of wind-driven hydrodynamics in lakes, we present here a detailed assessment of coastal landforms around two lakes in northeastern China and Mongolia.

Lake Hulun and Lake Buir are two neighboring shallow lakes with similar shapes, orientations, and climate conditions (Li *et al.*, 2013). Both lakes show a great diversity of littoral landforms with a notably asymmetric distribution pattern in terms of the distribution of depositional systems around the shoreline. In addition, the types and spatial associations of littoral landforms show some similarities and differences between the two lakes. Understanding where and how hydrodynamics drive erosional and depositional processes around the lake is not only the precondition for reconstructing the morphodynamical history of these lakes, but also enables us to simulate and predict scenarios of the lake's future (Cohen, 2003; Allen, 2008; Parsons and Abrahams, 2009; May *et al.*, 2022; Ohara *et al.*, 2022).

Most studies on Lake Hulun and Lake Buir so far have focused on the structural geology and aquatic environment (Xiao *et al.*, 2009; Li *et al.*, 2013, 2017, 2019; Wang *et al.*, 2015; Chen *et al.*, 2021), and there are only a few studies concerning the geomorphology, sedimentary facies, or hydrodynamics of the two lakes (Xia *et al.*, 2018; Fan *et al.*, 2021). Identifying the larger-scale distribution of lakes, and particularly their shape and morphologic patterns, is extremely difficult from the ground (Scheffers and Kelletat, 2016). Satellite images are playing an increasingly important role in the study of lake sedimentology, topography, and hydrodynamics (Schuster and Nutz, 2018; Chen *et al.*, 2020; Choudhury *et al.*, 2022; Gawehn *et al.*, 2022). Therefore, in this paper, we investigate the landform characteristics and facies distribution of these two wind-driven lakes based on the analysis of high-resolution satellite imagery and outcrop photos. The particular morphology of these littoral landforms helped reconstruct, from place to place, the main direction of clastic sediment transport. A sedimentary conceptual model is then proposed to account for the mapped landforms and their spatial arrangement. We then interpret the lake morphodynamics as well as the spatially and temporally varying influences of waves and currents on sediment transport pathways. Wind field and sediment supply are discussed as the dominant driving factors controlling the landforms and facies distribution in these lakes, thus providing a framework for facies recognition and prediction in other similar sedimentary basins around the world.

2. Study area

Lake Hulun and Lake Buir are two similarly shaped lakes located at the boundary between China and Mongolia (Fig. 1A and B). The shape of these two lakes is similar to a rectangle with rounded angles. They are lakes formed over time by collecting river discharge in half-graben basins (Chen *et al.*, 2007; Alexander *et al.*, 2022). The long axis of these two lakes is oriented SSW-NNE. Lake Buir receives an inflow from the Khalkh River that enters the lake in the northeast (Fig. 1B) and also has an outflow (the Orshuun River) that flows into Lake Hulun and connects the ~40 m higher Lake Buir to Lake Hulun (Fig. 1A, B and D). In addition, the Kherlen River flows into Lake Hulun from the southwest, and the Xinkai River flows into Lake Hulun from the northeast. The Xinkai River was built in the channel of the Dalaneluomu River in 1971 (Fig. 1B) to regulate the water level of Lake Hulun.

The annual average temperature of the region of Lake Hulun and Lake Buir (Fig. 1A) is 0.7 °C. The lowest temperature is in January, with an average temperature of −21.6 °C (Fig. 1C). The warmest month of the year is July, with an average temperature of 21.9 °C. The duration of ice coverage on the lakes and rivers typically spans from November to March (Fig. 1C). The average wind direction both in the ice period (November through March) and the ice-free period (April through October) is from the northwest (Fig. 1 E, F).

Today, Lake Hulun (117°E-117°50′E, 48°30′-49°20′N) has an area of 2339 km^2. The maximum water depth is

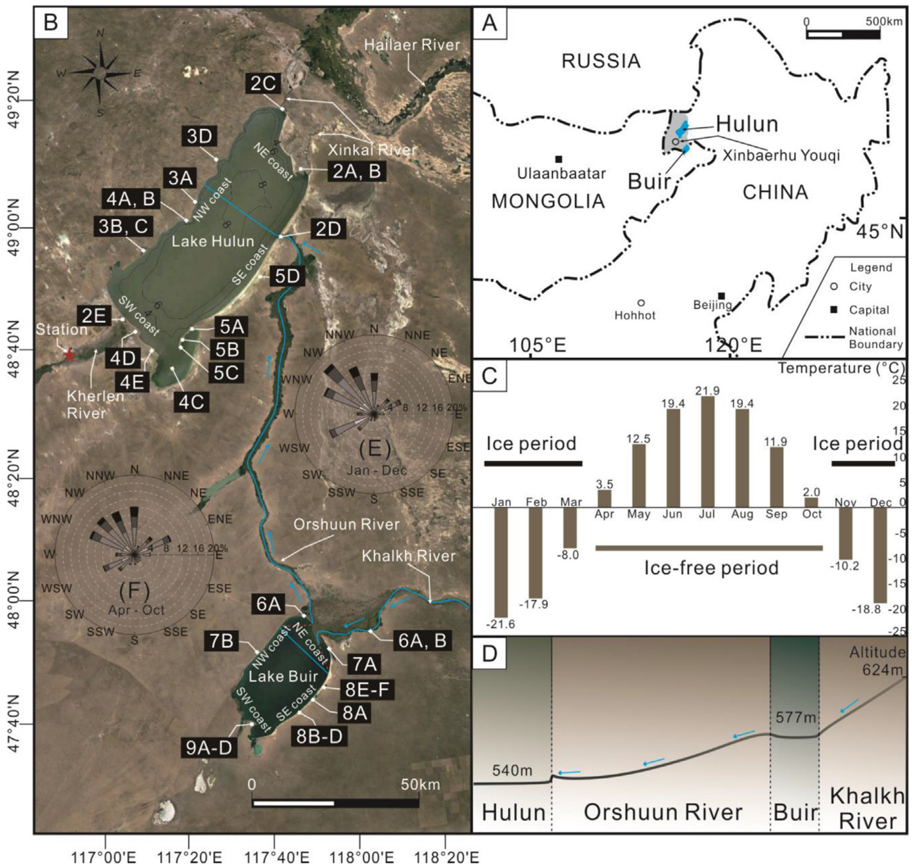

Fig. 1 **A)** Location of Lake Hulun and Lake Buir; **B)** Satellite view of Lake Hulun and Lake Buir and their main drainage network; **C)** The average temperature per month of Xinbaerhu Youqi from January 2010 to June 2021; **D)** The altitude along the Khalkh River - Lake Buir - Orshuun River - Lake Hulun (indicated by the blue line); **E)** The wind rose of Xinbaerhu Youqi from 2010 to 2021; **F)** The wind rose of Xinbaerhu Youqi between April and October from 2010 to 2021. The wind speed was the average speed per day. The shades from light to dark color reflect wind speed classes (0—2.5, 2.5—5.0, 5.0—7.5, and >7.5 m/s). The bathymetry of Lake Hulun is from Fan *et al.*, (2021). Temperature and wind data are from Xinbaerhu Youqi station (marked with a red star in figure B).

about 8 m, and the average water depth is about 5.7 m (Xia et al., 2018). Depending on fluctuating water levels, the lake was freshwater (salt content <1000 mg/L; most of the time) or brackish water (salt content <3500 mg/L) (Guo et al., 2022). Lake Hulun is about 75 km long in the NE direction and 28 km wide in the NW direction, with a length-width ratio of 2.7. The altitude of Lake Hulun is about 540 m (Fig. 1D).

Lake Buir (117°28′-117°54′E, 47°35′-47°59′N) is 35 km long and 20 km wide, with an area of 608.78 km^2 (Fig. 1B). Lake Buir has similar landforms to Lake Hulun. The length-width ratio is about 1.8. The lake is fresh water with an average depth of about 6 m, and the deepest depth of the lake can reach 10 m (Alexander et al., 2022). The altitude of Lake Buir is about 577 m (Fig. 1D).

3. Methodology

Freely available satellite images (from Google Earth) were used to document, map, describe, and analyze the landforms around Lake Hulun and Lake Buir in this paper. In addition, a field survey for Lake Buir was carried out to check mapping results and assess sedimentary facies around the shoreline. Photos of outcrops were analyzed and combined with satellite images to determine the characteristics, distribution pattern, and hydrodynamics of the sediments. Weather data, including wind direction, wind speed, and temperature, were taken from the station of Xinbaerhu Youqi in China (www.cma.gov.cn). The elevation variation from Lake Hulun to Lake Buir was analyzed using Google Earth. The factors controlling the geomorphological and sedimentological characteristics were then discussed.

To describe their geometry, the center of each lake was taken as the coordinate origin, and the lakes were divided into four sides and four corners, including two long segments (southeastern and northwestern coasts), two short segments (southwestern and northeastern coasts), two acute angles (northern and southern corners), and two obtuse angles (western and eastern corners). Due to the prevailing northwest wind, the southeastern lake margin is defined as the downwind (leeward) side of the lake, and the northwestern lake margin is defined as the upwind (windward) side.

The fetch for a particular location is estimated by constructing a series of 15 radiating lines at 6° intervals and extending these lines to a distant shoreline (Håkanson and Jansson, 1983; Gilbert, 1999). The lengths of these lines are measured and then averaged according to the cosine of the angle to estimate the fetch. The effective fetch is given by:

$$F_e = \Sigma f_i \cos \alpha_i / \Sigma \cos \alpha$$

Where f_i is the distance to the nearest shore along radials at α = 0°, ±6, ±12°, ..., ±42°.

Finally, the I_{wwb} index (the wind fetch (km) to average water depth (m) ratio; see Nutz et al., 2018) is referred to in this paper to quantitatively identify these two lakes as wind-driven water bodies. The larger the I_{wwb} value, the stronger the effect of wind-wave transformation on the lake sediments is (Nutz et al., 2018). When the I_{wwb} value is greater than 3.0, the lake belongs to a wind-driven water body. The I_{wwb} of Lake Hulun is about 4.4 (fetch = 25.1 km; average water depth = 5.7 m), while the I_{wwb} of Lake Buir (fetch = 19.6 km; average water depth = 6.0 m) is about 3.2. Both lakes are thus considered wind-driven water bodies.

4. Results

4.1. *Littoral landforms at Lake Hulun*

4.1.1. Wave-influenced river delta

In addition to the three largest rivers (Xinkai River, Orshuun River, and Kherien River), there are ca. eighty smaller streams that flow into Lake Hulun (Xia et al., 2018). They all have the potential to form river deltas.

The Xinkai River has two main channels (Fig. 1B). The eastern one flows into the lake from the southern part of the delta (Fig. 2A). The estuary shows an irregular zigzag-shaped landform, which looks like it has been affected by waves (Fig. 2A and B). The lake-facing side of the delta was reworked into barrier spits (Fig. 2A). A spit and bay formed in the southern part of the delta (Fig. 2B). The western channel of the Xinkai River shows a barrier island landform at the estuary (Fig. 2C), that may have been formed by the redistribution of waves.

The Orshuun River enters Lake Hulun from the southeast (Fig. 2D). A distributary channel and underwater bar show a directional change to southwest shoreline parallel after the river enters the lake (Fig. 2D).

The Kherien River flows into Lake Hulun from the southwest (Fig. 2E). Floodplains developed around the channels of the Kherien River (Fig. 2E) which may have

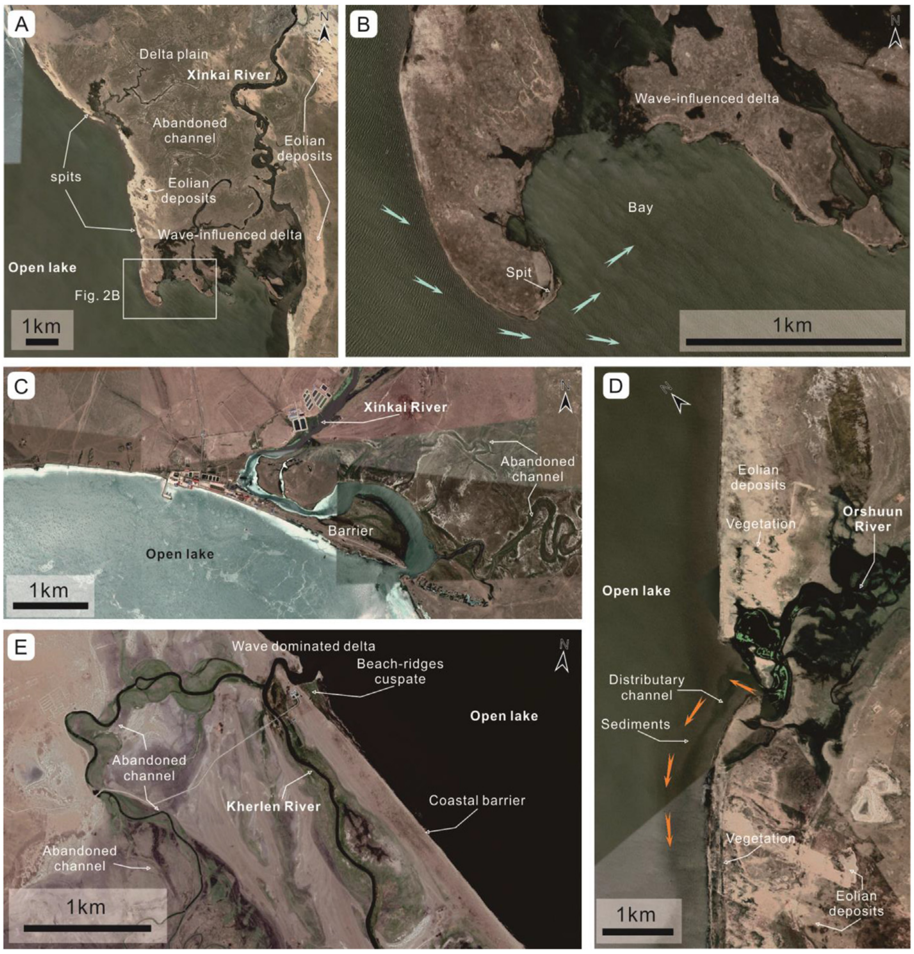

Fig. 2 Wave-influenced delta of Lake Hulun. **A)** Eastern channel of the Xinkai River; spits formed on the west edge of the delta; some eolian deposits with an NW—SE extension direction developed behind the beach and around the river; **B)** The southern part of the delta; **C)** Western channel of the Xinkai River; barrier island landform; **D)** The Orshuun River in the east of Lake Hulun; some eolian deposits were distributed behind the beach; **E)** The Kherlen River in the south of Lake Hulun; beach-ridges cuspate.

been created by river migration. A cuspate landform developed at the Kherien River mouth (Fig. 2E) which was formed by a prograding series of beach ridges.

4.1.2. Wave-influenced fan delta

Alluvial fans develop in front of a scarp on the northwestern shores of Lake Hulun (Fig. 3A—C). Some small-scale gullies serve as important sediment transport channels for alluvial fans. Alluvial deposits could cross and cover beach-ridges on the shore (Fig. 3C). Some inactive braided channels and alluvial fans are distributed behind the shore (Fig. 3B, D, and 4A). Barriers developed in front of the fan delta (Fig. 3A). They could be shore-parallel beach bars or barrier spits. These barriers may derive from wave-modified sediments of the fan delta and some short and straight seasonal streams.

4.1.3. Beach and spits

The beach deposits on the northwestern shore mainly derive from some ephemeral streams (Fig. 3A—C) and the erosion of the scarp (Fig. 3G). With about 50—700 m, the beach along the southeastern shore (Fig. 2D and 5D) is wider than the northwestern beach (about 3—50 m; Fig. 3C and 4B). Some beach-ridges developed along two headlands, forming barriers and lagoons (Fig. 3D—F). Sediments derived from a short stream (about 1500 m) on the northwestern lake margin could be redeposited by waves along the shore, forming a beach-ridges cuspate (Fig. 4B).

Spits are created by the process of longshore drift (Krist and Schaetzl, 2001; Bouchette *et al.*, 2014; Schuster *et al.*, 2014; Schuster and Nutz, 2018). Sediments carried by longshore drifts deposit when the velocity decreases, which often occurs where the

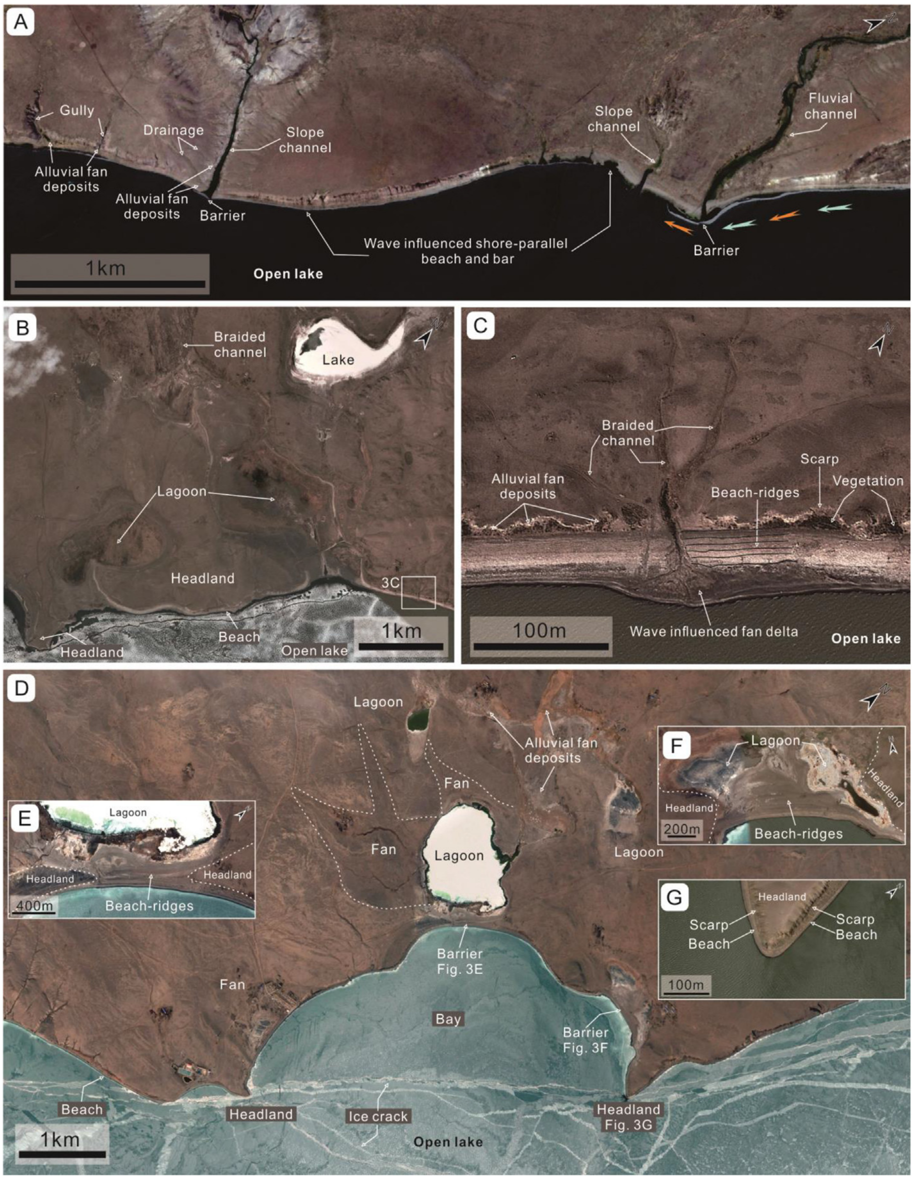

Fig. 3 The landforms of the NW coast. **A)** Alluvial fans in front of the scarp; short and straight channels; barriers formed at the river mouth; **B)** Braided channels; the front of the headland was modified to beach deposits; **C)** Fan delta deposits were transformed into beach deposits; **D)** The bay between two headlands; alluvial fan and fan delta deposits; **E-F)** The barrier formed between two headlands; **G)** The beach deposits in front of the scarp.

coastline breaks, e.g., at headlands or river mouths (Kunte and Wagle, 1991; Aagaard *et al.*, 2007). The sediment accumulation along the headland of the northwestern lake margin formed a large cuspate spit, about 1 km in width, that was made up of a sequence of beach-ridges (Fig. 4A). The short side of the cuspate spit is the erosional side, and the long side is the depositing side. Braided rivers are observed behind this big cuspate spit (Fig. 4A).

There are three main spits in the southern corner of Lake Hulun (Fig. 4C). Two of them are on the southwestern coast and show a series of hooks (Fig. 4D and E). The length of these two spits is about 4—7 km. The frontal part of the spits curves inwards towards the land, forming hooks for the waves that push the sediments toward the shore (Ashton *et al.*, 2016). Salt marshes develop behind the hooks because the spit offers protection from the stronger waves and the wind, allowing salt-tolerant plants to grow (Fig. 4D and E) (Redfield, 1965; Schuster and Nutz, 2018).

The spit on the southeastern lake margin is about 9 km long. It has a complex structure (Fig. 5A—C). Barrier spits developed on the northern part of the bay

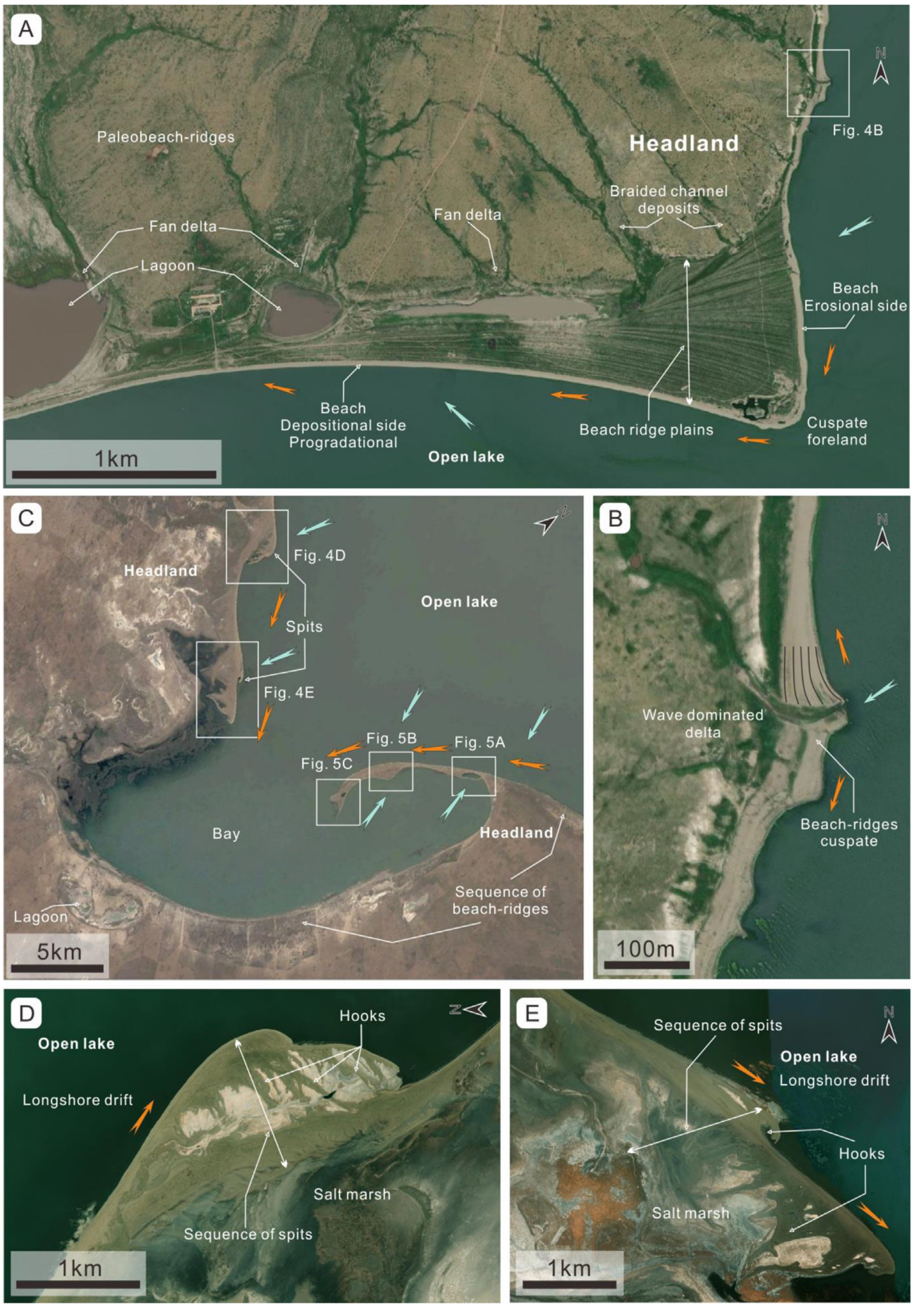

Fig. 4 Spits of Lake Hulun. **A)** Cuspate spit at the NW coast; beach ridge plains; **B)** Beach-ridges cuspate; **C)** Spits in the southern angle of Lake Hulun; **D-E)** Spits at the SW coast; salt marshes formed behind the spits.

side, which means there are two sediment transport directions (Fig. 5A). A cuspate spit developed in the middle of the bay margin, with a sequence of beach ridges indicating a northward longshore drift (Fig. 5B). There is a lagoon and beach-ridge sequence at the outer part of the large spit, which indicates a southward longshore drift (Fig. 5C). In combination, these indicate a complex hydrodynamic situation along the bay margin.

4.1.4. Eolian deposits and landforms

Eolian deposits are mainly developed on the backshore of the eastern shoreline of Lake Hulun in the form of a kilometer-wide coastal dunes system, including foredune ridges, blowouts, and parabolic and barchan dunes (Fig. 2D and 5D). Some eolian deposits also appear on the delta plain in the north of the lake (Fig. 2A). The shapes of both the parabolic and the

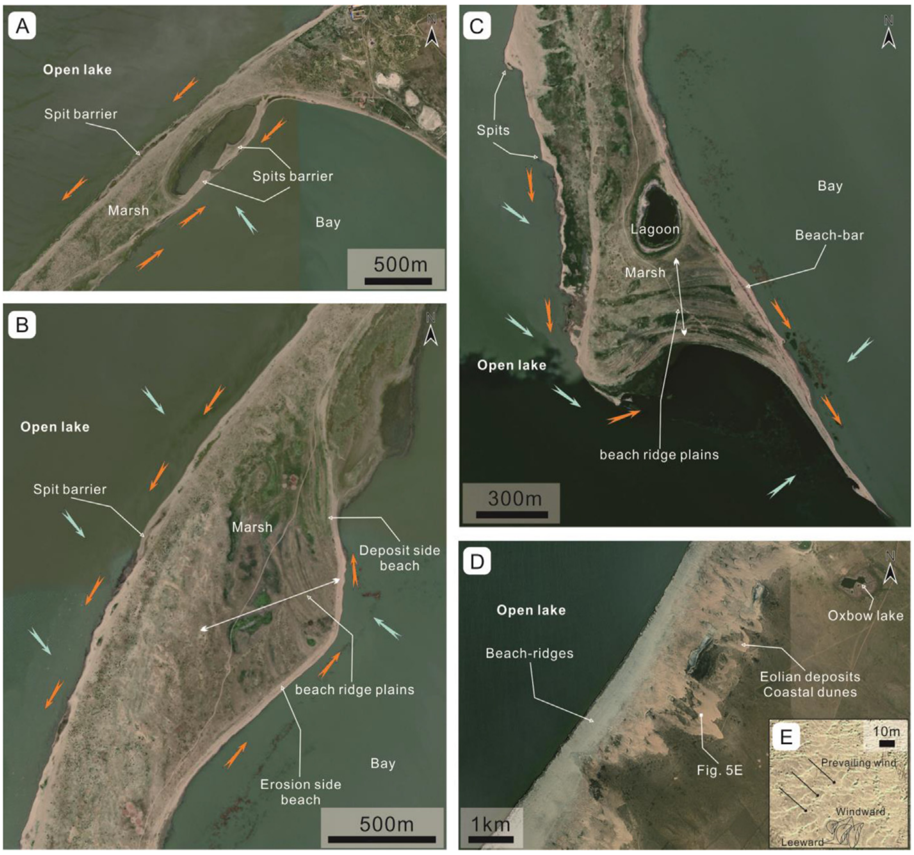

Fig. 5 Spits and eolian deposits at the SE coast of Lake Hulun. **A)** Spits barrier; **B)** Cuspate spit; beach ridge plains at the bay side; **C)** Some small spits at the lake side; beach ridge plains at the outer part of the big spit; **D)** Beach deposits at the SE coast and the eolian deposits behind the beach; **E)** Barchan dunes indicating the prevailing wind direction.

barchan dunes indicate a dominant wind direction from the northwest toward the southeast (Fig. 5E), which is consistent with our statistics of wind directions from 2010 to 2021 (Fig. 1E).

4.2. Littoral landforms at Lake Buir

4.2.1. Wave-influenced river delta

The Khalkh River is a meandering river that forms a large delta on the northern shore of Lake Buir (Fig. 6A and B). The floodplain is about 280 km^2 with many abandoned channels. On the floodplain and river cutbanks, dense vegetation grows (Fig. 6A and B). Exposed sandy deposits are distributed along the river (Fig. 6B). The sandy deposits are dominated by fine to medium sand with silt and clay mixed with some plant debris.

The extensional direction of the ca. 3300 m long delta is from NW to SE (Fig. 6A). The shape of the delta front reveals a strong influence from waves. Multiple nearshore bars with a width of about 50–600 m are distributed parallel to the shore (Fig. 6C and D). There is a remarkable series of beach-ridges developed over a width of 1100 m in the western part of the delta (Fig. 6A) which may reflect the progradation of the shoreline (Otvos, 2000).

4.2.2. Beach and spits

Beach deposits are widely distributed along the coast, whereas spits are primarily at the southern angle of Lake Buir (Figs. 7–9). The width of the southeastern beach is about 20–40 m (Fig. 7A), while the width of the northwestern beach is about 4–20 m (Fig. 7B).

Some beach cusps develop on the shoreface (Fig. 7C and D). The scarp behind the southeastern beach is approximately 10 m high and is made up of sandstones with parallel bedding, cross-bedding, and massive bedding (Fig. 7E and F). The erosion of scarp sandstones likely provides material for beach deposits. Beach deposits are composed of sand and sand mixed with mud and organic matter (Fig. 8B–D). The nearshore bars appear clearly on the satellite images during the ice period (Fig. 8A, A′). There are about ten crests of linear nearshore bars distributed over a 300 m wide area (Fig. 8A’).

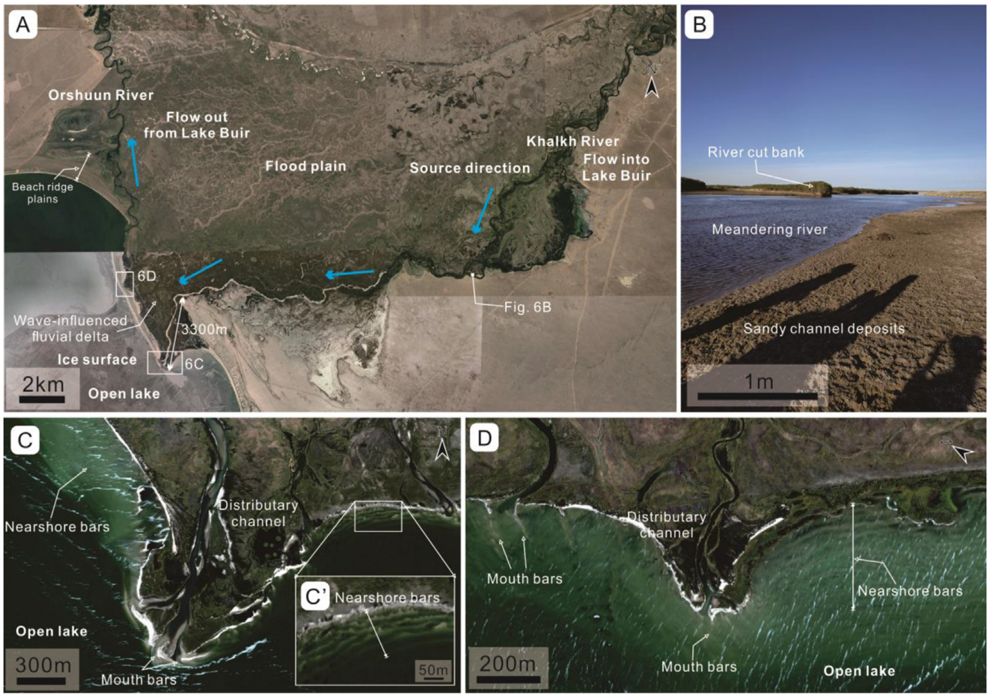

Fig. 6 Wave-influenced delta of Lake Buir. **A)** Floodplains distributed in north of Lake Buir; the Khalkh River flows into Lake Buir, and the Orshuun River flows out from Lake Buir; beach ridge plains distributed at the side of the delta front; **B)** Cut-bank and exposed sandy channel deposits along the Khalkh River; **C-D)** Mouth bars; nearshore bars.

If a spit extends from a headland to another headland or two opposite spits connect, then a barrier will form. The spits on the southeastern and southwestern shores of Lake Buir are linked, forming two isolated lagoons (Fig. 9A). There are also spits that are progressively evolving and may merge in the future (Fig. 9B), eventually forming a new barrier and a new lagoon.

The spit, with a length of about 850 m, extends into the lake and thus has a bay side and lake side (Fig. 9C). Currents and waves along the bay side are weaker and form muddy beach deposits (Fig. 9D), while the lakeside has stronger waves and currents and forms sandy beach deposits (Fig. 9E). On the lake side, a beach ridge and swale are observed (Fig. 9E). At the head of the spit, a sandy bar and a small lagoon are forming (Fig. 9F). Under the action of onshore waves and longshore currents, the sandy bar will gradually move closer to the shore, possibly transforming into beach deposits. The resulting series of beach-ridges has a width of about 210 m (Fig. 9C).

4.2.3. Eolian deposits and landforms

A large area of eolian landforms and deposits, with a width of about 300—1500 m, developed behind the beach in the southeastern part of Lake Buir (Fig. 8A). The extensional direction of eolian sands is mainly from northwest to southeast, which confirms the dominant role of the northwesterly wind in the formation of eolian deposits (Fig. 8A).

Eolian dunes and dune grass can be seen behind the beach (Fig. 8B and C). Wind ripples develop on the eolian sands, which are dominated by well-sorted, rounded, or subrounded fine sand (Fig. 8E and F). There are also some grass dunes and wind ripples that could be seen on the beach (Fig. 7E). The scarp prevented some beach sands from being blown by the northwesterly wind, and the beach sands were transformed into an eolian landform at the bottom of the scarp (Fig. 7E).

5. Discussion

5.1. The relationship between littoral landforms, wind field, provenance, hydrodynamics, and sediment distribution

Lake Hulun and Lake Buir have the same shape and are similarly oriented to the prevailing wind direction. Although there are some differences in the configuration of these two lakes, they strikingly develop similar littoral landforms at similar locations. This strongly suggests a primary control of hydro-sedimentary processes by wind forcing.

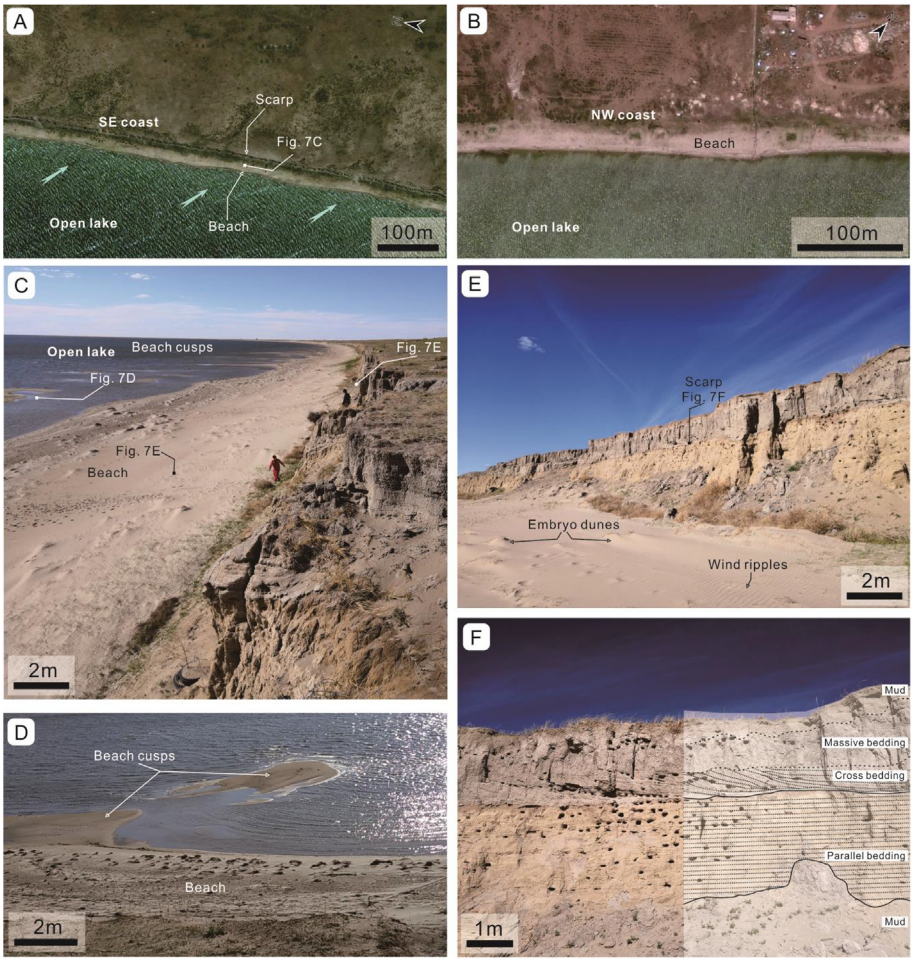

Fig. 7 Beach deposits of Lake Buir. **A)** Beach in front of the scarp on the SE coast; **B)** Beach at the NW coast; **C)** The field photo of the beach and scarp; beach cusps; **D)** Beach cusps; **E)** Embryo dunes and wind ripples developed on the beach in front of the scarp; **F)** The sandstones of the scarp with parallel bedding, cross-bedding, and massive bedding; the sandstones may be the paleo-channel or paleo-shoreface deposits.

5.1.1. The similarity of landforms between Lake Hulun and Lake Buir

Lake Hulun and Lake Buir have the same extensional direction of spits and delta fronts. The main water and sediment supply to each of the lakes comes from an axial river that enters the waterbody from the northeastern short coast segments, where two large wave-influenced deltas form. And the resulting delta fronts have the same extensional direction of NW to SE, likely influenced by an NW—SE longshore current (Fig. 10). Spits on the SW shores of both lakes also exhibit the same extensional directions (Fig. 10). Spits on the SE shore have an extensional direction of NE to SW that indicates a longshore drift from NE to SW. One important characteristic of these two lakes is that remarkable spits are well developed at similar locations for both lakes.

The beach and eolian deposits of two lakes are more developed on the SE coast. Both lakes have a large and dominantly sandy beach and a dune field that developed downwind from the SE coast of the lake, likely providing evidence for the effects of prevailing northwestern winds on lacustrine littoral landforms and dynamics (Fig. 10). Because the northwesterly wind is also dominant throughout the non-ice period (Fig. 1F), a large area of beach sand is formed by wind-waves on the southeastern shores, which is then the source of sand for the coastal dunes (Fig. 2D and 5D). The extension of dunes also indicates the source of eolian deposits and implies that they are beach-fed. Elevation increases from the lakes' downwind coast towards the east (Fig. 1D), facilitating the deposition and stabilization of these eolian deposits.

The reason why eolian dunes developed on the SE coast but not on the NW coast of lakes has been interpreted as the result of the northwest prevailing winds and the abundant vegetation on the NW coast (Ji *et al.*, 1994; Li *et al.*, 2009; Cui *et al.*, 2015; Xia *et al.*, 2018). This is generally confirmed by the fact that the beach in the NW area of the two lakes has a much smaller width

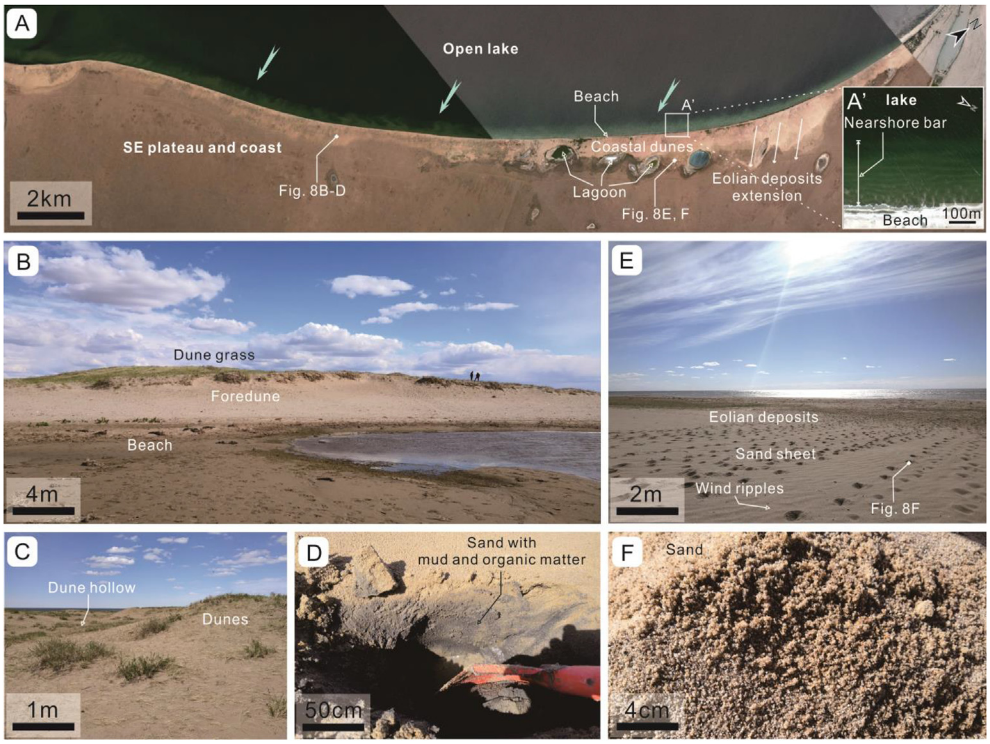

Fig. 8 Beach and eolian deposits at the SE coast of Lake Buir. **A)** The landforms of the SE coast; A': nearshore bars distributed in front of the beach; **B)** Foredune and dune grass behind the beach; **C)** Dunes and dune hollows; grass dunes; **D)** Beach deposits; yellow fine and silt sand at the top; silt, mud, and organic matter mixed at the bottom; **E)** A large area of eolian deposits with the topography of the Gobi Desert; wind ripples; **F)** The sands of the Gobi Desert are well-rounded, and the grain size ranges from fine sand to coarse sand.

than the beach in the SE area, indicating that wind-wave action is weaker on the upwind NW shore.

Multiple nearshore bars are well developed in lakes. Nearshore bars are formed by the combined action of onshore and offshore currents (Dally *et al.*, 1984; Gallagher *et al.*, 1998; Eichentopf *et al.*, 2019). Nearshore bars migrate either onshore or offshore as a result of wave intensity, water depth, and slope change (Ruessink and Terwindt, 2000; Chen and Dodd, 2021). The multiple nearshore bars in Lake Buir are formed possibly due to the fact that the water level of lakes in the study area has been rising since 2012 (Li *et al.*, 2019; Alexander *et al.*, 2022), which preserves onshore migrating bars at different depths (Różyński and Lin, 2015; Splinter *et al.*, 2018). Although there are no applicable satellite images to observe nearshore bars in Lake Hulun, we speculate that nearshore bars also exist underwater in Lake Hulun.

5.1.2. The difference in landforms between Lake Hulun and Lake Buir

More beach and eolian deposits are found in Lake Hulun. The beach and eolian deposits of Lake Hulun are generally larger than those on Lake Buir (Fig. 10), which may result from the longer fetch, shallower water depth, and higher sediment supply of Lake Hulun compared to Lake Buir. When the water is deep enough, the size of the waves is proportional to the wind fetch in an enclosed lake system (Håkanson and Jansson, 1983). The shallower the water in the downwind area, the easier it is for the waves to interact with the lakebed and rework sediments (Reading and Collinson, 1996; Rafiuddin *et al.*, 2010; Peters and Loss, 2012). In addition, the Orshuun River discharged into Lake Hulun from the southeast coast and brought some sediments into the lake which did not happen in Lake Buir. So, on the downwind coast of Lake Hulun, there will be larger waves reworking more sediments than in Lake Buir.

Eolian deposits are only found on the floodplain north of Lake Hulun. There are some eolian deposits distributed adjacent to the rivers of the northern delta plain of Lake Hulun (Fig. 2A). However, no eolian deposits are found in relation to the river associated with the northern delta of Lake Buir, which is possibly due to the Khalkh River's flood regime causing a dense plant cover on its floodplain (Fig. 6A). In contrast, the Xinkai River and dams built to regulate the level of Lake Hulun have reduced the possibility of flooding. As a result, some abandoned river deposits are exposed and transformed into eolian deposits.

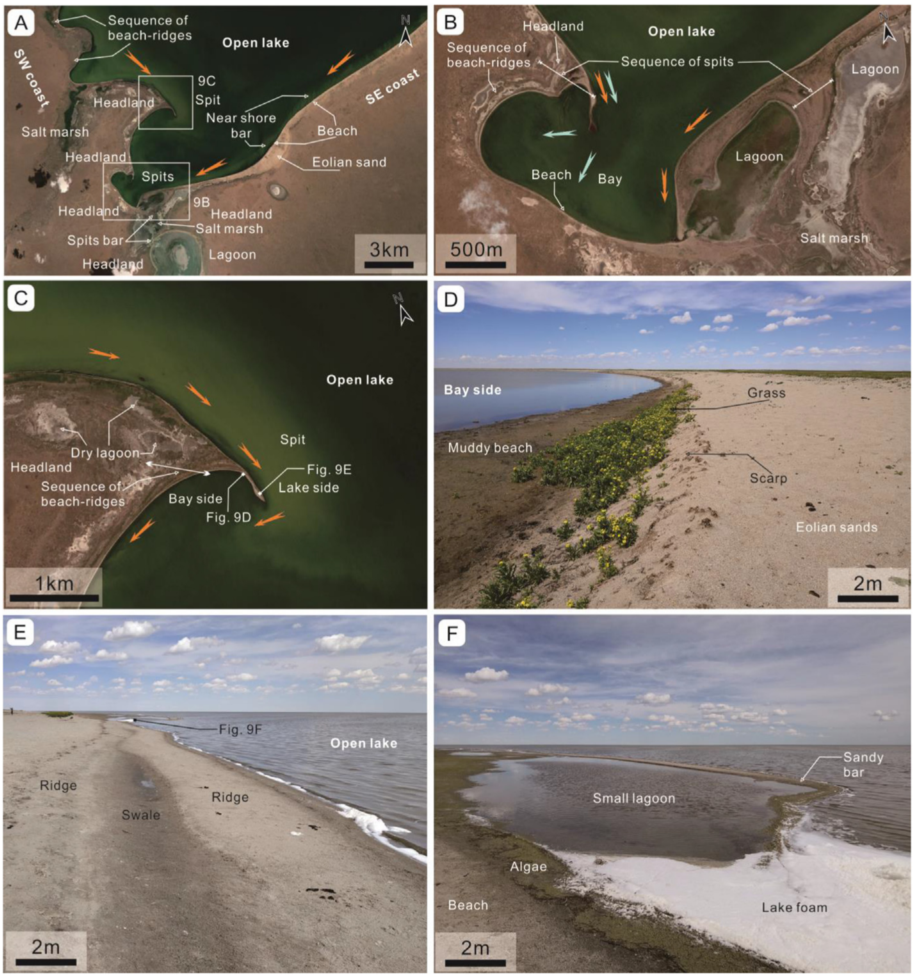

Fig. 9 Spits at the southern corner of Lake Buir. **A)** The landforms of the southern corner; spits at the SW and SE coasts; spit barriers and lagoons; **B)** Closed and unclosed spits; **C)** The spit at the SW coast; **D)** The bay side of the spit; muddy beaches; sandy scarps and grasses behind the beach; **E)** The lake side of the spit; ridges and swales; **F)** The front part of the spit; a sandy bar and a small lagoon.

The development of alluvial fans and fan deltas in the NW area of Lake Hulun was likely influenced by geomorphological and topographical processes related to tectonic movements (Chen *et al.*, 2007; Xia *et al.*, 2018). In contrast to Lake Hulun, the NW area of Lake Buir is flat, with no interpreted local-scale uplift. So, there is more sediment supply on Lake Hulun's NW than that on Lake Buir. Alluvial fans form on the northwest coast of Lake Hulun as a result of episodic or temporal flooding which did not occur in Lake Buir.

The deltas in Lake Hulun are significantly different in scale. The deltas on the northeast coast are larger than the deltas on the southwest coast of Lake Hulun; they have the same fetch under NW winds. And the bathymetry of Fan *et al.* (2021) shows that there is very little difference between the northeastern and southwestern areas of the lake. Thus, we assume that the influences of waves and longshore currents on deltas are the same, which means that the sediment supply of the Xinkai River is much greater than that of the Kherien River. There are possibly two reasons why the Orshuun River on the southeastern coast of Lake Hulun has not formed a delta. Firstly, the wave reworking effect on the southeastern coast is very strong. Secondly, the Orshuun River flows through a short and heavily vegetated area, so it doesn't carry a lot of sediments.

The landforms distributions are similar in Lake Hulun and Lake Buir but are different in scale. And Lake Hulun has more landform types, such as fan deltas, which are not developed in Lake Buir. Based on the analysis of these similarities and differences, we concluded that the landforms of the lakes are mainly controlled by wind fields and sediment supply. According to our observations of landforms along Lake Hulun and Lake Buir and the interpreted longshore drift directions, we propose a conceptual model for wind-driven water bodies for which the wind direction

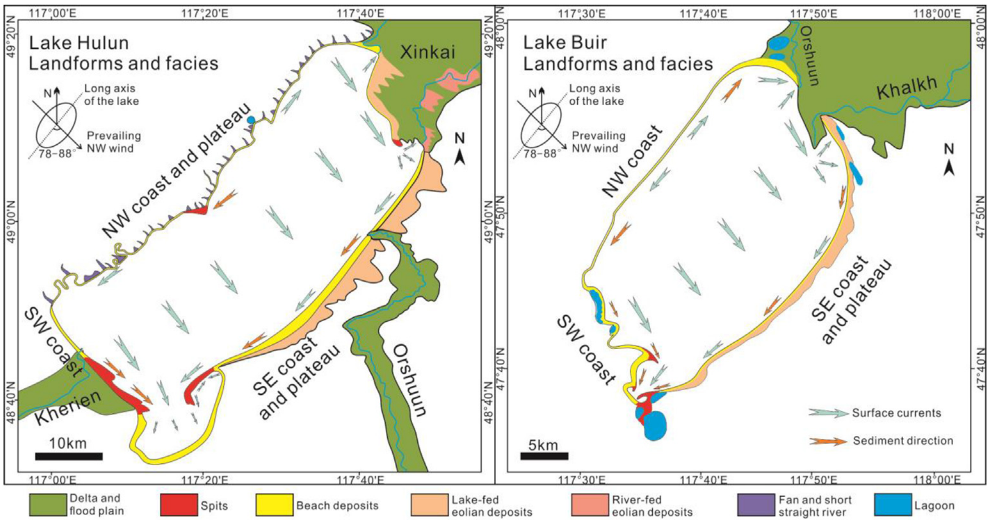

Fig. 10 Landforms map of Lake Hulun and Lake Buir. The current direction and sediment direction are inferred from the prevailing NW winds and topographic features.

is nearly perpendicular to the long axis of rectangular-shaped lakes.

5.2. A conceptual sedimentary model of Lake Hulun and Lake Buir

In conventional lacustrine depositional models, wind forcing is recognized but largely viewed as subordinate to fluvial drivers (Johnson, 1984; Dam and Surlyk, 1992; Carroll and Bohacs, 1999). In accordance with some other recent studies (Bouchette *et al.*, 2010; Nutz *et al.*, 2015, 2018; Zăinescu *et al.*, 2023), we demonstrate here that wind forcing is the dominant factor influencing the littoral lacustrine sedimentary system of Lake Hulun and Lake Buir. The prevailing wind blows from the northwest, which has a cross-angle of about 78—88° with the SE coast (long axis of lakes).

Waves created by the prevailing wind mainly travel from the upwind to the downwind shores of the lakes. Most of the energy of wave and wind is therefore released along the downwind lake margin (SE coast), forming a wide beach and beach-fed eolian dunes beyond (Fig. 11), and causing a general asymmetry in the distribution of littoral landforms around the lakes. Nearshore bars generate when sediment-laden backflow resulting from wave breaking on the shoreface intersects with the onshore current at a specific location (Fig. 11). Rivers are the main source of clastic sediments for these two lakes, and the resulting deltas show clear geomorphological evidence for modification by waves in varying degrees. Some littoral landforms are also eroded and serve as sediment sources.

The growth direction of spits is the same as the longshore current direction (Krist and Schaetzl, 2001; Bouchette *et al.*, 2014; Schuster *et al.*, 2014). Longshore currents near the SW and NE coasts have a NW—SE direction, and longshore currents near the SE coast have a NE—SW direction (Fig. 11). NW—SE longshore currents from upwind to downwind must therefore have influenced the delta extending to the downwind side while forming spits on the southwestern coast. The NE—SW longshore current forms a spit at the southern end of the downwind coast. For the cross-angle (78—88°) of the NW prevailing wind and the downwind coast, the longshore current along the downwind coast is mainly from north to south. Spits in the southern corner are easily connected to form spit barriers and lagoons for the accumulation of sediments carried by longshore drifts (Fig. 11).

The accumulation of waves on the downwind side of the lakes will raise the water level on the SE coast, generating a bottom current to move from the downwind side to the upwind side (Robert and Imberger, 1980; Monismith, 1985; Bouchette *et al.*, 2010). Where the longshore currents converge, the currents from different directions meet to produce downwelling (Chikita, 1992; Botte and Kay, 2002), also forming reverse bottom currents in the southern lake corner (Fig. 11). Where the bottom currents flow back toward the upwind shore area, an upwelling reconnects the bottom currents to the surface currents (Csanady, 1982; Nutz *et al.*, 2015). The bottom currents originate from the downwelling flow to the upwind side to form a wind-driven water circulation together with upwelling and surface currents. Such a model of wind-driven hydrodynamics has recently

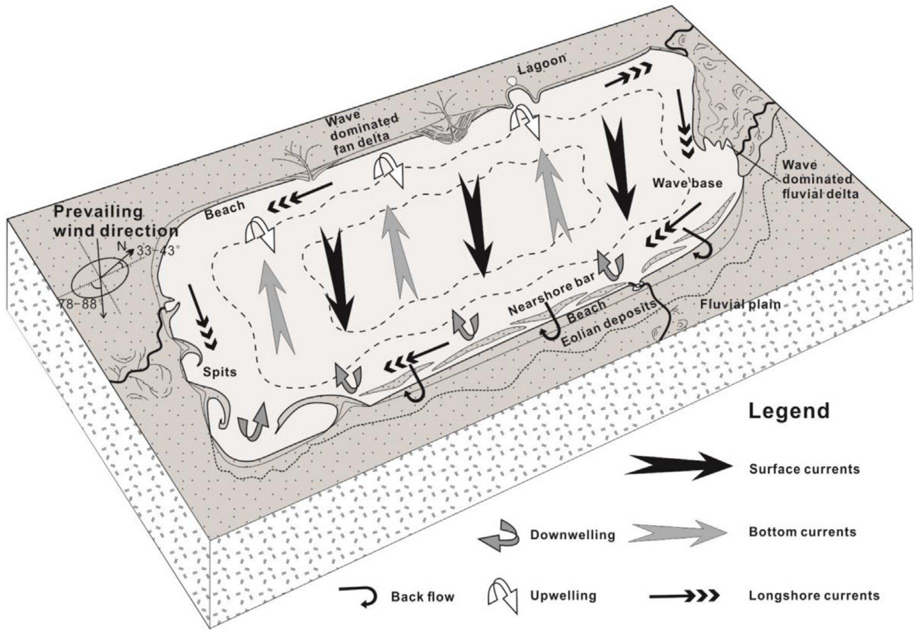

Fig. 11 Sedimentary model related to wind-driven water circulation under the prevailing wind in a rectangular-shaped rift lake basin based on Lake Hulun and Lake Buir.

been supported by the simulation of current azimuths and velocities for Megalake Chad (Bouchette *et al.*, 2010), Lake Saint-Jean (Nutz *et al.*, 2015), and Lake Turkana (Zăinescu *et al.*, 2023).

Preserved lacustrine beach and nearshore bar deposits are potentially high-quality subsurface reservoirs (Jiang, 2018) and have been described in the Dongying Depression (Wang *et al.*, 2018), Gaoyou Sag (Liu *et al.*, 2021), and Tanan Depression (Xue *et al.*, 2021). Defining the palaeowind characteristics and building the appropriate sedimentary model are the keys to determining the distribution pattern of beach-bar sandbodies (Wang *et al.*, 2018; Jiang, 2018). The sedimentary model proposed in this paper, based on modern wind-wave controlled lakes, may provide a good reference for building subsurface geomodels of wind-wave controlled lacustrine strata.

6. Conclusions

Lake Hulun and Lake Buir provide two new examples of wind-driven lakes. These two lakes present a similar shape and orientation to the dominant wind direction, and the littoral landforms developed around these lakes show a great similarity.

1) The main littoral landforms developing in these two lakes are beaches, beach-ridges, spits, wave-influenced deltas, and eolian deposits. All these geomorphic features reveal a strong influence of wind, forcing the transport and redistribution of clastics in lacustrine sedimentary systems, dominantly not only in the water body (subaqueous processes) but also around it (subaerial processes). Sediment supply to the basin is also a major parameter to be considered, as reflected by the morphological differences between the deltas developing in these two lakes.
2) Beach and eolian deposits are dominant on the downwind coast. The progradation of the delta front and spits on the NE coast and SW coast is affected by longshore currents that extend in the downwind direction and run almost parallel to the short coast segments. The longshore currents mainly flow to the south end of the downwind coast along a 78–88° cross-angle relative to the NW prevailing wind and downwind coast, which forms spits at the southern part of the SE coast. The spits at the SW and SE coasts preferentially merge, generating barriers and lagoons at the southern corner.
3) A generic conceptual model is proposed to present the wind-driven hydro-sedimentary dynamics occurring in lakes that share the same main characteristics as lakes Hulun and Buir, namely a rectangular water body with a prevailing wind that is almost perpendicular to its long axis (i.e., a lake with an upwind and a downwind shore and two along wind shores). The surface currents caused by the prevailing wind will accumulate on the downwind side, where they will

converge with the longshore currents, forming downwelling. The resulting bottom currents will flow toward the upwind area to form a wind-driven water circulation with the upwelling and surface currents. With this model, the resulting distribution of clastic deposits and landforms can now be forecasted for similar configurations, especially the resulting differences between the upwind and the downwind shores of the water body.

4) Based on two natural case studies, this paper examines the main sedimentary geomorphology and discusses the hydrodynamics in the context of the dominant wind direction, but it does not discuss the influence of other possible wind directions (e.g., opposite alternating wind directions, parallel to the long axis, etc.), which will be explored in the future. The main littoral landforms correspond well to the dominant wind forcing and provide a robust first-order understanding of hydrodynamics.

Declaration of competing interest

There is no conflict of interest to declare.

Acknowledgements

We thank the technical experts of Tamsag Mongolia (XIX) Company who participated in the field survey of Lake Buir for providing a really good understanding of the lake's landforms and sedimentary characteristics. This work was supported by the National Science and Technology Special Project (No. 2017ZX05009-002) and the Fundamental Research Funds for the Central Universities. FZ was supported by CNES through the funding of his postdoctoral fellowship.

References

Aagaard, T., Orford, J., Murray, A.S., 2007. Environmental controls on coastal dune formation; Skallingen Spit, Denmark. *Geomorphology*, 83, 29—47. https://doi.org/10.1016/j.geomorph.2006.06.007.

Alexander, O., Munkhjargal, U., Tuyagerel, D., 2022. *Lakes of Mongolia Geomorphology, Geochemistry and Paleoclimatology*. Springer, Cham, pp. 103—113. https://doi.org/10.1007/978-3-030-99120-3.

Allan, J.C., Kirk, R.M., 2000. Wind wave characteristics at Lake Dunstan, South Island, New Zealand. *New Zealand Journal of Marine & Freshwater Research*, 34, 573—591. https://doi.org/10.1080/00288330.2000.9516959.

Allen, P.A., 2008. From landscapes into geological history. *Nature*, 451, 274—276. https://doi.org/10.1038/nature06586.

Andrews, S.D., Hartley, A.J., 2015. The response of lake margin sedimentary systems to climatically driven lake level fluctuations: Middle Devonian, Orcadian Basin, Scotland. *Sedimentology*, 62, 1693—1716. https://doi.org/10.1111/sed.12200.

Ashton, A., Nienhuis, J., Ells, K., 2016. On a neck, on a spit: controls on the shape of free spits. *Earth Surface Dynamics*, 4, 193—210. https://doi.org/10.5194/esurf-4-193-2016.

Botte, V., Kay, A., 2002. A model of the wind-driven circulation in Lake Baikal. *Dynamics of Atmospheres and Oceans*, 35, 131—152. https://doi.org/10.1016/S0377-0265(01)00086-0.

Bouchette, F., Mathieu, S., Jean-Francois, G., Clea, D., Claude, R., Abderamane, M., Patrick, M., Duringer, P., 2010. Hydrodynamics in Holocene Lake Mega-Chad. *Quaternary Research*, 73, 226—236. https://doi.org/10.1016/j.yqres.2009.10.010.

Bouchette, F., Manna, M., Montalvo, P., Nutz, A., Schuster, M., Ghienne, J.-F., 2014. Growth of cuspate spits. *Journal of Coastal Research*, 70, 47—52. https://doi.org/10.2112/si70-009.1.

Carroll, A.R., Bohacs, K.M., 1999. Stratigraphic classification of ancient lakes: Balancing tectonic and climatic controls. *Geology*, 27, 99—102. https://doi.org/10.1130/0091-7613(1999)027<0099:Scoalb>2.3.Co;2.

Carson, C., Hussey, K.M., 1962. The oriented lakes of Arctic Alaska. *The Journal of Geology*, 70(4), 417—439. https://doi.org/10.1086/626834.

Chen, J., Jiang, Z., Zhang, W., Liu, C., Han, C., 2020. The study on the modern sedimentary system of Buha River Delta in Qinghai Lake. *Geological Journal*, 55, 5216—5232. https://doi.org/10.1002/gj.3735.

Chen, J.L., Wu, H.Y., Zhu, D.F., Lin, C.H., Yu, D.S., 2007. Tectonic evolution of the Hailar Basin and its potentials of oil-gas exploration. *Chinese Journal of Geology*, 1, 147—159 (In Chinese with English abstract).

Chen, W.L., Dodd, N., 2021. A nonlinear perturbation study of a shoreface nourishment on a multiply barred beach. *Continental Shelf Research*, 214, 104317. https://doi.org/10.1016/j.csr.2020.104317.

Chikita, K., 1992. The role of sediment-laden underflows in lake sedimentation: Glacier-fed Peyto Lake, Canada. *Journal of the Faculty of Science, Hokkaido University - Series 7: Geophysics*, 9(2), 211—224. http://hdl.handle.net/2115/8784.

Choudhury, S., Phukan, S., Duarah, B.P., Goswami, D.C., Mehta, M., 2022. Glacier inventory of the Subansiri River Basin in the Brahmaputra catchment using Landsat satellite data: A case study of the Daisaphu Glacier changes. *Geological Journal*, 57(12), 4939—4954. https://doi.org/10.1002/gj.4403.

Clifton, H.E., 2006. A Reexamination of Facies Models for Clastic Shorelines. In: Posamentier, H.W., Walker, R.G. (Eds.), *Facies Models Revisited*. SEPM Society for

Sedimentary Geology, Oklahoma, pp. 293—337. Special Publication no. (2006).

Cohen, A.S., 2003. *Paleolimnology: The History and Evolution of Lake Systems*. Oxford University Press, New York, p. 528.

Csanady, G., 1982. On the structure of transient upwelling events. *Journal of Physical Oceanography*, 12(1), 84—96. https://doi.org/10.1175/1520-0485(1982)012<0084:OTSOTU>2.0.CO;2.

Cui, X.Y., Yang, J., Hao, J.X., Bu, T.G., Liu, Z.G., 2015. The history and evolution of Hulun Lake. *Inner Mongolia Science Technology & Economy*, 1, 43—47 (In Chinese with English abstract).

Dally, W.R., Dean, R.G., Asce, M., 1984. Suspended sediment transport and beach profile evolution. *Journal of Waterway, Port, Coastal, and Ocean Engineering*, 110(1), 15—33. https://doi.org/10.1061/(ASCE)0733-950X(1984)110:1(15).

Dam, G., Surlyk, F., 1992. Forced regressions in a large wave- and storm-dominated anoxic lake, Rhaetian-Sinemurian Kap Stewart Formation, East Greenland. *Geology*, 20, 749—752. https://doi.org/10.1130/0091-7613(1992)020<0749:Frialw>2.3.Co;2.

Davis, R.A., Hayes, M.O., 1984. What is a wave-dominated coast? *Marine Geology*, 60(1—4), 313—329. https://doi.org/10.1016/0025-3227(84)90155-5.

Eichentopf, S., Van Der Zanden, J., Cáceres, I., Alsina, J.M., 2019. Beach profile evolution towards equilibrium from varying initial morphologies. *Journal of Marine Science and Engineering*, 7, 406. https://doi.org/10.3390/jmse7110406.

Fan, C., Song, C., Liu, K., Ke, L., Xue, B., Chen, T., Fu, C., Cheng, J., 2021. Century-scale reconstruction of water storage changes of the largest lake in the Inner Mongolia Plateau using a machine learning approach. *Water Resources Research*, 57(2), e2020WR028831. https://doi.org/10.1029/2020wr028831.

Gallagher, E.L., Elgar, S., Guza, R., 1998. Observations of sand bar evolution on a natural beach. *Journal of Geophysical Research: Oceans*, 103, 3203—3215. https://doi.org/10.1029/97JC02765.

Gawehn, M., Almar, R., Bergsma, E.W.J., de Vries, S., Aarninkhof, S., 2022. Depth inversion from wave frequencies in temporally augmented satellite video. *Remote Sensing*, 14(8), 1847. https://doi.org/10.3390/rs14081847.

Gilbert, R., 1999. Calculated wave base in relation to the observed patterns of sediment deposition in Northeastern Lake Ontario. *Journal of Great Lakes Research*, 25, 883—891. https://doi.org/10.1016/S0380-1330(99)70785-9.

Guo, J., Zhang, Y., Shi, X., Sun, B., Wu, L., Wang, W., 2022. Driving mechanisms of the evolution and ecological water demand of Hulun Lake in Inner Mongolia. *Water*, 14(21), 3415. https://doi.org/10.3390/w14213415.

Håkanson, L., Jansson, M., 1983. Principles of Lake Sedimentology . *Caldwell*. The Blackburn Press, New Jersey, p. 316. https://doi.org/10.1007/978-3-642-69274-1.

Ji, L., Xia, W., Xiang, L., Wang, S., 1994. Mineral composition and sedimentation rate of surficial sediments in Hulun Lake, Inner Mongolia. *Journal of Lake Sciences*, 3, 227—232.

Jiang, Z., 2018. Wind-Source-Basin Sedimentary System: Elements and Research Methods of Sedimentary Dynamics of Windfield. *Source-Basin System*. Springer Singapore, Singapore, pp. 29—40. https://doi.org/10.1007/978-981-10-7407-3_2.

Jiang, Z., Wang, J., Fulthorpe, C.S., Liu, L., Zhang, Y., Liu, H., 2018. A quantitative model of paleowind reconstruction using subsurface lacustrine longshore bar deposits — An attempt. *Sedimentary Geology*, 371, 1—15. https://doi.org/10.1016/j.sedgeo.2018.04.004.

Johnson, T.C., 1984. Sedimentation in large lakes. *Annual Review of Earth and Planetary Sciences*, 12, 179—204. https://doi.org/10.1146/annurev.ea.12.050184.001143.

Keighley, D., 2008. A lacustrine shoreface succession in the Albert Formation, Moncton Basin, New Brunswick. *Bulletin of Canadian Petroleum Geology*, 56, 235—258. https://doi.org/10.2113/gscpgbull.56.4.235.

Krist, F., Schaetzl, R.J., 2001. Paleowind (11,000 BP) directions derived from lake spits in Northern Michigan. *Geomorphology*, 38, 1—18. https://doi.org/10.1016/S0169-555X(00)00040-4.

Kunte, P.D., Wagle, B., 1991. Spit evolution and shore drift direction along South Karnataka coast, India. *Giornale di Geologia*, 153, 71—80.

Li, C., Sun, B., Jia, K., Zhang, S., Li, W., Shi, X., Cordovil, C.M.d.S., Pereira, L.S., 2013. Multi-band remote sensing based retrieval model and 3D analysis of water depth in Hulun Lake, China. *Mathematical and Computer Modelling*, 58, 771—781. https://doi.org/10.1016/j.mcm.2012.12.027.

Li, C., Wang, J., Hu, R., Yin, S., Bao, Y., Li, Y., 2017. ICESat/GLAS-derived changes in the water level of Hulun Lake, Inner Mongolia, from 2003 to 2009. *Frontiers of Earth Science*, 12(2), 420—430. https://doi.org/10.1007/s11707-017-0666-8.

Li, S., Chen, J., Xiang, J., Pan, Y., Huang, Z., Wu, Y., 2019. Water level changes of Hulun Lake in Inner Mongolia derived from Jason satellite data. *Journal of Visual Communication and Image Representation*, 58, 565—575. https://doi.org/10.1016/j.jvcir.2018.12.031.

Li, X., Bao, S., Chang, S., Bai, M., 2009. Analysis on the cause of formation of zonal dune of Hulun Lake area in Inner Mongolia. *Meteorology Journal of Inner Mongolia*, 3, 30—31.

Liu, C., Jiang, Z., Zhou, X., Duan, Y., Lei, H., Wang, X., Atuquaye Quaye, J., 2021. Paleocene storm-related event beds in the Gaoyou Sag of the Subei Basin, eastern China: A new interpretation for these deep lacustrine sandstones. *Marine and Petroleum Geology*, 124, 104850. https://doi.org/10.1016/j.marpetgeo.2020.104850.

May, J.-H., May, S.M., Marx, S.K., Cohen, T.J., Schuster, M., Sims, A., 2022. Towards understanding desert shorelines - coastal landforms and dynamics around ephemeral Lake Eyre North, South Australia. *Transactions of the Royal Society of South Australia*, 146, 59—89. https://doi.org/10.1080/03721426.2022.2050506.

Monismith, S.G., 1985. Wind-forced motions in stratified lakes and their effect on mixed-layer shear. *Limnology* *and Oceanography*, 30, 771—783. https://doi.org/10.4319/lo.1985.30.4.0771.

Nordstrom, K.F., Jackson, N.L., 2012. Physical processes and landforms on beaches in short fetch environments in estuaries, small lakes and reservoirs: A review. *Earth-Science Reviews*, 111, 232—247. https://doi.org/10.1016/j.earscirev.2011.12.004.

Nutz, A., Schuster, M., Ghienne, J.F., Roquin, C., Hay, M.B., Rétif, F., Certain, R., Robin, N., Raynal, O., Cousineau, P.A., Team, S., Bouchette, F., 2015. Wind-driven bottom currents and related sedimentary bodies in Lake Saint-Jean (Québec, Canada). *Geological Society of America Bulletin*, 127, 1194—1208. https://doi.org/10.1130/b31145.1.

Nutz, A., Schuster, M., Ghienne, J.F., Roquin, C., Bouchette, F., 2018. Wind-driven waterbodies: a new category of lake within an alternative sedimentologically-based lake classification. *Journal of Paleolimnology*, 59, 189—199. https://doi.org/10.1007/s10933-016-9894-2.

Ohara, N., Jones, B.M., Parsekian, A.D., Hinkel, K.M., Yamatani, K., Kanevskiy, M., Rangel, R.C., Breen, A.L., Bergstedt, H., 2022. A new Stefan equation to characterize the evolution of thermokarst lake and talik geometry. *The Cryosphere*, 16, 1247—1264. https://doi.org/10.5194/tc-16-1247-2022.

Otvos, E.G., 2000. Beach ridges — definitions and significance. *Geomorphology*, 32(1), 83—108. https://doi.org/10.1016/S0169-555X(99)00075-6.

Parsons, A.J., Abrahams, A.D., 2009. *Geomorphology of Desert Environments*. Springer Netherlands, Dordrecht, pp. 3—12. https://doi.org/10.1007/978-1-4020-5719-9.

Peters, S.E., Loss, D.P., 2012. Storm and fair-weather wave base: A relevant distinction? *Geology*, 40, 511—514. https://doi.org/10.1130/g32791.1.

Pochat, S., Driessche, J.V.D., Mouton, V., Guillocheau, F., 2005. Identification of Permian palaeowind direction from wave-dominated lacustrine sediments (Lodeve Basin, France). *Sedimentology*, 52, 809—825. https://doi.org/10.1111/j.1365-3091.2005.00697.x.

Rafiuddin, A.M., Faizal, M., Prasad, K., Cho, Y.-J., Kim, C.-G., Lee, Y.-H., 2010. Exploiting the orbital motion of water particles for energy extraction from waves. *Journal of Mechanical Science and Technology*, 24, 943—949. https://doi.org/10.1007/s12206-010-0203-0.

Reading, H.G., Collinson, J.D., 1996. *Sedimentary Environments: Processes, Facies and Stratigraphy*. Blackwell Science, Oxford, UK, pp. 154—258.

Redfield, A.C., 1965. Ontogeny of a salt marsh estuary. *Science*, 147, 50—55.

Robert, H.S., Imberger, J., 1980. The classification of mixed-layer dynamics of lakes of small to medium size. *Journal of Physical Oceanography*, 10(7), 1104—1121.

Różyński, G., Lin, J.-G., 2015. Data-driven and theoretical beach equilibrium profiles: implications and consequences. *Journal of Waterway, Port, Coastal, and Ocean Engineering*, 141, 04015002. https://doi.org/10.1061/(ASCE)WW.1943-5460.0000304.

Ruessink, B., Terwindt, J., 2000. The behaviour of nearshore bars on the time scale of years: a conceptual model. *Marine Geology*, 163, 289—302. https://doi.org/10.1016/S0025-3227(99)00094-8.

Scheffers, A.M., Kelletat, D.H., 2016. *Lakes of the World with Google Earth: Understanding Our Environment*. Springer Nature, Switzerland, pp. 1—46. https://doi.org/10.1007/978-3-319-29617-3.

Schuster, M., Roquin, C., Duringer, P., Brunet, M., Caugy, M., Fontugne, M., Taïsso Mackaye, H., Vignaud, P., Ghienne, J.-F., 2005. Holocene Lake Mega-Chad palaeoshorelines from space. *Quaternary Science Reviews*, 24, 1821—1827. https://doi.org/10.1016/j.quascirev.2005.02.001.

Schuster, M., Roquin, C., Moussa, A., Ghienne, J., Duringer, P., Bouchette, F., Durand, A., Allenbach, B., 2014. Shorelines of the Holocene Megalake Chad (Africa, Sahara) investigated with very high resolution satellite imagery (Pléiades): example of the Goz Kerki paleo-spit. *Revue française de photogrammétrie et de télédétection*, 208, 63—68. https://doi.org/10.52638/rfpt.2014.114.

Schuster, M., Nutz, A., 2018. Lacustrine wave-dominated clastic shorelines: modern to ancient littoral landforms and deposits from the Lake Turkana Basin (East African Rift System, Kenya). *Journal of Paleolimnology*, 59, 221—243. https://doi.org/10.1007/s10933-017-9960-4.

Schwartz, R.K., 2012. Bedform, texture, and longshore bar development in response to combined storm wave and current dynamics in a nearshore helical flow system. *Journal of Coastal Research*, 28, 1512—1535. https://doi.org/10.2112/JCOASTRES-D-11-00102.1.

Splinter, K.D., Gonzalez, M.V., Oltman-Shay, J., Rutten, J., Holman, R., 2018. Observations and modelling of shoreline and multiple sandbar behaviour on a high-energy meso-tidal beach. *Continental Shelf Research*, 159, 33—45. https://doi.org/10.1016/j.csr.2018.03.010.

Wang, J., Jiang, Z., Xian, B., Chen, J., Wang, X., Xu, W., Liu, H., Dey, S., 2018. A method to define the palaeowind strength from lacustrine parameters. *Sedimentology*, 65, 461—491. https://doi.org/10.1111/sed.12388.

Wang, W., Liu, L., Ma, Y., He, J., 2015. Spatial distributions and environmental implications of diatom assemblages in surface sediments of Hulun Lake, China. *Environmental Earth Sciences*, 74, 1803—1813. https://doi.org/10.1007/s12665-015-4188-y.

Xia, S., Liu, Z., Liu, J., Chang, Y., Li, P., Gao, N., Ye, D., Wu, G., Yu, L., Qu, L., Tong, L., Li, S., 2018. The controlling factors of modern facies distributions in a half-graben lacustrine rift basin: A case study from Hulun Lake, Northeastern China. *Geological Journal*, 53, 977—991. https://doi.org/10.1002/gj.2938.

Xiao, J., Chang, Z., Wen, R., Zhai, D., Itoh, S., Lomtatidze, Z., 2009. Holocene weak monsoon intervals indicated by low lake levels at Hulun Lake in the monsoonal margin region of northeastern Inner Mongolia, China. *The Holocene*, 19, 899—908. https://doi.org/10.1177/0959683609336574.

Xue, X., Zhang, Y., Jiang, Z., Wang, L., Wang, S., Jiang, H., 2021. Wave and storm signals in a lacustrine succession and their relationship to paleowind direction (Tanan Depression, Mongolia, early Cretaceous). *Sedimentary Geology*, 419, 105911. https://doi.org/10.1016/j.sedgeo.2021.105911.

Zăinescu, F., van der Vegt, H., Storms, J., Nutz, A., Bozetti, G., May, J.-H., Cohen, S., Bouchette, F., May, S.M., Schuster, M., 2023. The role of wind-wave related processes in redistributing river-derived terrigenous sediments in Lake Turkana: A modelling study. *Journal of Great Lakes Research*, 49(2), 368—386. https://doi.org/10.1016/j.jglr.2022.12.013.

Li Wang is a PhD student of School of Energy Resources, China University of Geosciences (Beijing). His research interests are sedimentology, geomorphology, and oil exploration.

Mathieu Schuster is Senior Researcher (and Directeur de Recherche) of Centre National de la Recherche Scientifique (CNRS), Institut Terre et Environnement de Strasbourg, Université de Strasbourg, France. His research interests are hydrosystems of continental sedimentary basins.

Zai-Xing Jiang is Professor of School of Energy Resources, China University of Geosciences (Beijing). His research interests are sequence stratigraphy, sedimentology, reservoir geology, and oil and gas exploration.